CHAPTER ONE

Wireless Communication Links with Fading

The purpose of this chapter is to familiarize the reader with the basic propagation characteristics that describe various wireless communication channels, such as terrestrial, atmospheric, and ionospheric from VHF to the X-band. Well-known standards in wireless communication [1–10] are introduced for the prediction of path losses and fading effects of any radio signal in various communication links, and finally, new possibilities that can be obtained using smart antennas are discussed.

1.1. RADIO COMMUNICATION LINK

Different radio communication links (land, land-to-air, air-to-air) covering different atmospheric and ionospheric conditions include several components having a plethora of physical principles and processes, with their own independent or correlated working characteristics and operating elements. A simple scheme of such as a radio communication link consists of a transmitter (T), a receiver (R), and a propagation channel. The main output characteristics of such a link depend on the conditions of radio propagation in different kinds of environments, as shown in Figure 1.1. According to Reference 6, there are three main independent electronic and electromagnetic design tasks related to this wireless communication network. The first task is the transmitter antenna operation, including the specification of the electronic equipment that

Radio Propagation and Adaptive Antennas for Wireless Communication Networks: Terrestrial, Atmospheric, and Ionospheric, Second Edition. Nathan Blaunstein and Christos G. Christodoulou.

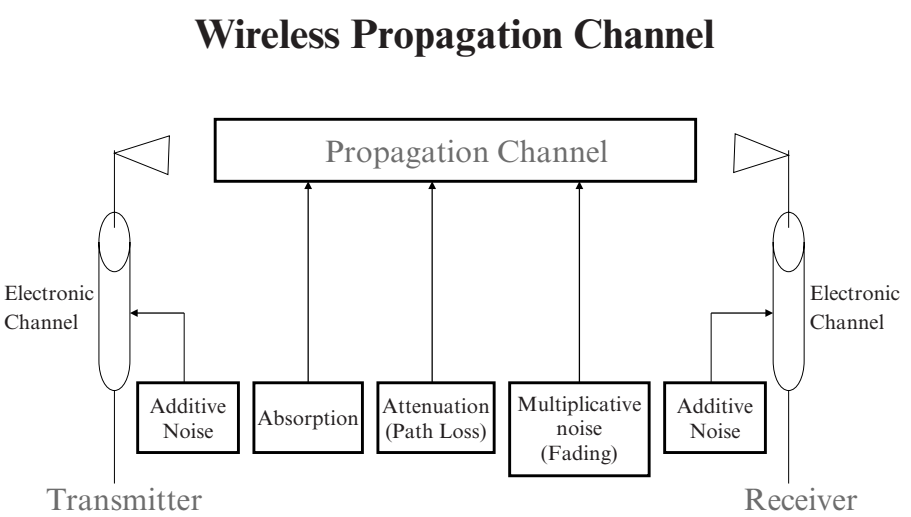

FIGURE 1.1. A wireless communication link scheme.

controls all operations within the transmitter. The second task is to understand, model, and analyze the propagation properties of the channel that connects the transmitting and receiving antennas. The third task concerns the study of all operations related to the receiver.

The propagation channel is influenced by the various obstructions surrounding antennas and the existing environmental conditions. Another important question for a personal receiver (or handheld) antenna is also the influence of the human body on the operating characteristics of the working antenna. The various blocks that comprise a propagation channel are shown in Figure 1.1.

Its main output characteristics depend on the conditions of radiowave propagation in the various operational environments where such wireless communication links are used. Next, we briefly describe the frequency spectrum, used in terrestrial, atmospheric, and ionospheric communications, and we classify some common parameters and characteristics of a radio signal, such as its path loss and fading for various situations which occur in practice.

1.2. FREQUENCY BAND FOR RADIO COMMUNICATIONS

The *frequency band* is a main characteristic for predicting the effectiveness of radio communication links that we consider here. The optimal frequency band for each propagation channel is determined and limited by the technical requirements of each communication system and by the conditions of radio

propagation through each channel. First, consider the spectrum of radio frequencies and their practical use in various communication channels [1–5].

Extremely low and *very low frequencies* (ELF and VLF) are frequencies below 3 kHz and from 3 kHz to 30 kHz, respectively. The VLF-band corresponds to waves, which propagate through the wave guide formed by the Earth's surface and the ionosphere, at long distances, with a low degree of attenuation (0.1–0.5 decibel (dB) per 1000 km [1–5]).

Low frequencies (LF) are frequencies from 30 kHz up to 3 MHz. In the 1950s and 1960s, they were used for radio communication with ships and aircraft, but since then they are used mainly with broadcasting stations. Because such radio waves propagate along the ground surface, they are called "surface" waves [1–5]. In terms of wavelength, we call these class of waves the *long* (from 30 kHz to 300 kHz) and *median* (from 300 kHz to 3 MHz) *waves*.

High frequencies (HF) are those which are located in the band from 3 MHz up to 30 MHz. Again, in the wavelength domain, we call these waves the *short waves*. Signals in this spectrum propagate by means of reflections caused by the ionospheric layers and are used for communication with aircrafts and satellites, and for long-distance land communication using broadcasting stations.

Very high frequencies (VHF) (or *short waves* in the wavelength domain) are located in the band from 30 MHz up to 300 MHz. They are usually used for TV communications, in long-range radar systems, and radio-navigation systems.

Ultra high frequencies (UHF) (*ultrashort waves* in the wavelength domain) are those that are located in the band from 300 MHz up to 3 GHz. This frequency band is very effective for wireless microwave links, constructions of cellular systems (fixed and mobile), mobile-satellite communication channels, medium-range radars, and other applications.

In recent decades, radio waves with frequencies higher than 3 GHz (C-, X-, K-bands, up to several hundred gigahertz, which in the literature are referred to as *microwaves* and *millimeter waves*), have begun to be widely used for constructing and performing modern wireless communication channels.

1.3. NOISE IN RADIO COMMUNICATION LINKS

The effectiveness of each radio communication link—land, atmospheric, or ionospheric—depends on such parameters as [9]:

- noise in the transmitter and in the receiver antennas
- noise within the electronic equipment that communicates with both antennas
- background and ambient noise (cosmic, atmospheric, artificial/man-made, etc.).

Now let us briefly consider each type of noise, which exists in a complete communication system. In a wireless channel, specifically, the noise sources can be subdivided into *additive* (or *white*) and *multiplicative* effects, as seen in Figure 1.1 [6, 7, 10].

The *additive noise* arises from noise generated within the receiver itself, such as thermal noise in passive and active elements of the electronic devices, and also from external sources such as atmospheric effects, cosmic radiation, and man-made noise. The clear and simple explanation of the first component of additive noise is that noise is generated within each element of the electronic communication channel due to the random motion of the electrons within the various components of the equipment [5]. According to the theory of thermodynamics, the noise energy can be determined by the average background temperature, T_0, as [1–5]

$$E_{\mathrm{N}} = k_{\mathrm{B}} T_0, \tag{1.1}$$

where

$$k_{\mathrm{B}} = 1.38 \times 10^{-23} W \times s \times K^{-1} \tag{1.2}$$

is Boltzman's constant, and $T_0 = 290$ K $= 17°$C. This energy is uniformly distributed in the frequency band and hence it is called "white noise." The total effective noise power at the receiver input is given by the following expression:

$$N_{\mathrm{F}} = k_{\mathrm{B}} T_0 B_{\mathrm{W}} F, \tag{1.3}$$

where F is the *noise figure* at the receiver and B_w is the bandwidth of the signal. The noise figure represents any additional noise effects related to the corresponding environment, and it is expressed as

$$F = 1 + \frac{T_e}{T_0}. \tag{1.4}$$

Here T_e is the effective temperature, which accounts for all ambient natural (weather, cosmic noise, clouds, rain, etc.) and man-made (industry, plants, power engine, power stations, etc.) effects.

The *multiplicative noise* arises from the various processes inside the propagation channel and depends mostly on the directional characteristics of both terminal antennas, on the reflection, absorption, scattering, and diffraction phenomena caused by various natural and artificial obstructions placed between and around the transmitter and the receiver (see Fig. 1.2). Usually, the multiplicative process in the propagation channel is divided into three types: *path loss*, *large-scale* (or *slow fading*), and *short-scale* (or *fast fading*)

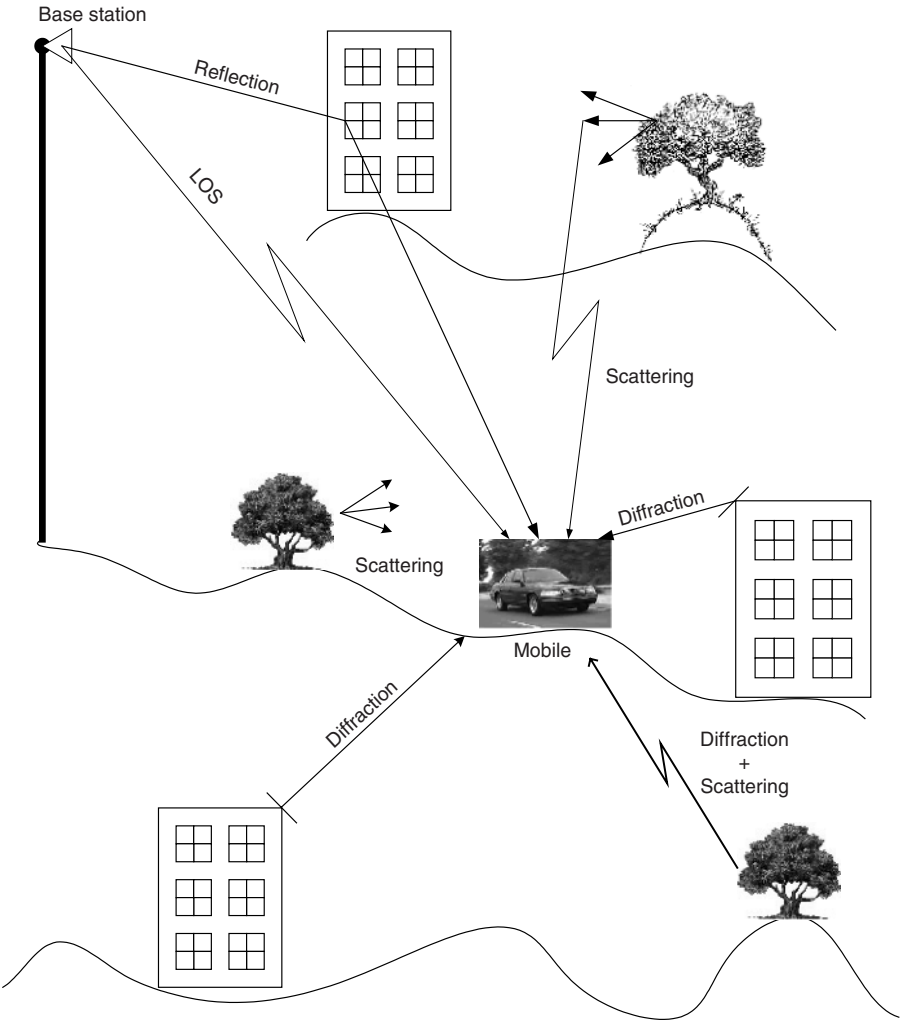

FIGURE 1.2. Multipath effects caused by various natural and artificial obstructions placed between and around the transmitting and the receiving antennas.

[7–10]. We describe these three characteristics of the multiplicative noise separately in the following section.

1.4. MAIN PROPAGATION CHARACTERISTICS

In real communication channels, the field that forms the complicated interference picture of received radio waves arrives via several paths simultaneously,

forming a multipath situation. Such waves combine vectorially to give an oscillating resultant signal whose variations depend on the distribution of phases among the incoming total signal components. The signal amplitude variations are known as the *fading* effect [1–4, 6–10]. Fading is basically a spatial phenomenon, but spatial signal variations are experienced, according to the ergodic theorem [11, 12], as temporal variations by a receiver/transmitter moving through the multipath field or due to the motion of scatterers, such as a truck, aircraft, helicopter, satellite, and so on. Thus, we can talk here about space-domain and time-domain variations of EM fields in different radio environments, as well as in the frequency domain. Hence, if we consider mobile, mobile-to-aircraft or mobile-to-satellite communication links, we may observe the effects of random fading in the frequency domain, that is, the complicated interference picture of the received signal caused by receiver/transmitter movements, which is defined as the "Doppler shift" effect [1–7, 10].

Numerous theoretical and experimental investigations in such conditions have shown that the spatial and temporal variations of signal level have a triple nature [1–7, 10]. The first one is the *path loss*, which can be defined as a large-scale smooth decrease in signal strength with distance between two terminals, mainly the transmitter and the receiver. The physical processes which cause these phenomena are the spreading of electromagnetic waves radiated outward in space by the transmitter antenna and the obstructing effects of any natural or man-made objects in the vicinity of the antenna. The spatial and temporal variations of the signal path loss are large and slow, respectively.

Large-scale (in the space domain) or *slow* (in the time domain) fading is the second nature of signal variations and is caused by diffraction from the obstructions placed along the radio link surrounding the terminal antennas. Sometimes this fading phenomenon is called the *shadowing effect* [6, 7, 10].

During shadow fading, the signal's slow random variations follow either a Gaussian distribution or a log-normal distribution if the signal fading is expressed in decibels. The spatial scale of these slow variations depends on the dimensions of the obstructions, that is, from several to several tens of meters. The variations of the total EM field describe its structure within the shadow zones and are called *slow-fading* signals.

The third nature of signal variations is the *short-scale* (in the space domain) or *fast* (in the time domain) signal variations, which are caused by the mutual interference of the wave components in the multiray field. The characteristic scale of such waves in the space domain varies from half wavelength to three wavelengths. Therefore, these signals are usually called *fast-fading* signals.

1.4.1. Path Loss

The path loss is a figure of merit that determines the effectiveness of the propagation channel in different environments. It defines variations of the signal amplitude or field intensity along the propagation trajectory (*path*) from

one point to another within the communication channel. In general [1–3, 6–10], the *path loss* is defined as a logarithmic difference between the amplitude or the intensity (called *power*) at any two different points, $\mathbf{r}_1$ (the transmitter point) and $\mathbf{r}_2$ (the receiver point), along the propagation path in the medium. The path loss, which is denoted by L and is measured in decibels, can be evaluated as follows [5]:

for a signal amplitude of $A(\mathbf{r}_j)$ at two points $\mathbf{r}_1$ and $\mathbf{r}_2$ along the propagation path

$$L = 10 \cdot \log \frac{A^2(\mathbf{r}_2)}{A^2(\mathbf{r}_1)} = 10 \cdot \log A^2(\mathbf{r}_2) - 10 \cdot \log A^2(\mathbf{r}_1)$$
$$= 20 \cdot \log A(\mathbf{r}_2) - 20 \cdot \log A(\mathbf{r}_1)\,[\text{dB}]; \tag{1.5}$$

for a signal intensity $J(\mathbf{r}_j)$ at two points $\mathbf{r}_1$ and $\mathbf{r}_2$ along the propagation path

$$L = 10 \cdot \log \frac{J(\mathbf{r}_2)}{J(\mathbf{r}_1)} = 10 \cdot \log J(\mathbf{r}_2) - 10 \cdot \log J(\mathbf{r}_1)\,[\text{dB}]. \tag{1.6}$$

If we assume now $A(\mathbf{r}_1) = 1$ at the transmitter, then

$$L = 20 \cdot \log A(\mathbf{r})\,[\text{dB}] \tag{1.7a}$$

and

$$L = 10 \cdot \log J(\mathbf{r})\,[\text{dB}]. \tag{1.7b}$$

For more details about how to measure the path loss, the reader is referred to References 1–3 and 6–10. As any signal passing through the propagation channel passes through the transmitter electronic channel and the receiver electronic channel (see Fig. 1.1), both electronic channels together with the environment introduce additive or white noise into the wireless communication system. Therefore, the second main figure of merit of radio communication channels is the signal-to-noise ratio (SNR or S/N). In decibels this SNR can be written as

$$\text{SNR} = P_{\text{R}} - N_{\text{R}}\ [\text{dB}], \tag{1.8}$$

where P_{R} is the signal power at the receiver, and N_{R} is the noise power at the receiver.

1.4.2. Characteristics of Multipath Propagation

Here we start with the general description of *slow* and *fast* fading.

Slow Fading. As was mentioned earlier, the *slow* spatial signal variations (expressed in decibels) tend to have a log-normal distribution or a Gaussian

distribution (expressed in watts [W]) [1–4, 6–10]. The *probability density function* (PDF) of the signal variations with the corresponding standard deviation, averaged within some individual small area or over some specific time period, depends on the nature of the terrain, of the atmospheric and ionospheric conditions. This PDF is given by [1–4]

$$\mathrm{PDF}(r) = \frac{1}{\sigma_L \sqrt{2\pi}} \exp\left\{-\frac{(r-\overline{r})^2}{2\sigma_L^2}\right\}. \tag{1.9a}$$

The corresponding *cumulative distributed function* (CDF) (or the total probability itself) is given by [1–4]

$$CDF(Z) \equiv \Pr(r < Z) = \int_0^Z PDF(r)dr. \tag{1.9b}$$

Here $\overline{r} = \langle r \rangle$ is the mean value of the random signal level, r is the value of the received signal strength or voltage envelope, $\sigma_L = \langle r^2 - \overline{r}^2 \rangle$ is the variance or time-average power ($\langle \mathrm{r} \rangle$ indicates the averaging operation of a variable r of the received signal envelope), and Z is the slow fade margin giving maximum effect of slow fading on the signal envelope slow variations. Usually, slow fading, described by a Gaussian PDF or CDF, can be presented via the Q-function defined as a *complementary cumulative distribution function* (CCDF) [11, 12]

$$Q(Z) \equiv CCDF(Z) = 1 - CDF(Z) \equiv \Pr(r > Z) \tag{1.10}$$

In References 11 and 12, it was shown that this function is closely related to the so-called error function, $\mathrm{erf}(w)$, usually used in description of the stochastic processes in probability theory and in statistical mechanics:

$$Q(w) = \frac{1}{\sqrt{2\pi}} \int_{x=w}^{\infty} \exp\left\{-\frac{x^2}{2}\right\} dx = \frac{1}{2}\mathrm{erf}\left\{\frac{w}{\sqrt{2}}\right\}$$

and

$$\mathrm{erf}(w) = \frac{2}{\sqrt{\pi}} \int_0^w \exp(-y^2)dy.$$

Fast Fading. For the case of stationary receiver and transmitter (*static multipath channel*), due to multiple reflections and scattering from various obstructions surrounding the transmitter and receiver, the radio signals travel along different paths of varying lengths, causing such fast deviations of the signal strength (in volts) or power (in watts) at the receiver.

In the case of a *dynamic multipath* situation, either the subscribers' antenna is in movement or the objects surrounding the stationary antennas are moving, so the spatial variations of the resultant signal at the receiver can be seen as temporal variations [11, 12]. The signal received by the mobile at any spatial point may consist of a large number of signals having randomly distributed amplitudes, phases, and angles of arrival, as well as different time delays. All these features change the relative phase shifts as a function of the spatial location and, finally, cause the signal to fade in the space domain. In a dynamic (mobile) multipath situation, the signal fading at the mobile receiver occurs in the time domain. This temporal fading is associated with a shift of frequency radiated by the stationary transmitter. In fact, the time variations, or dynamic changes of the propagation path lengths, are related to the Doppler effect, which is due to relative movements between a stationary base station (BS) and a moving subscriber (MS).

To illustrate the effects of phase change in the time domain due to the Doppler frequency shift (called the Doppler effect [1–4, 6–10]), let us consider a mobile moving at a constant velocity v, along the path XY, as shown in Figure 1.3. The difference in path lengths traveled by a signal from source S to the mobile at points X and Y is $\Delta\ell = \ell\cos\theta = \nu\Delta t\cos\theta$, where Δt is the time required for the moving receiver to travel from point X to Y along the path, and θ is the angle between the mobile direction along XY and direction to the

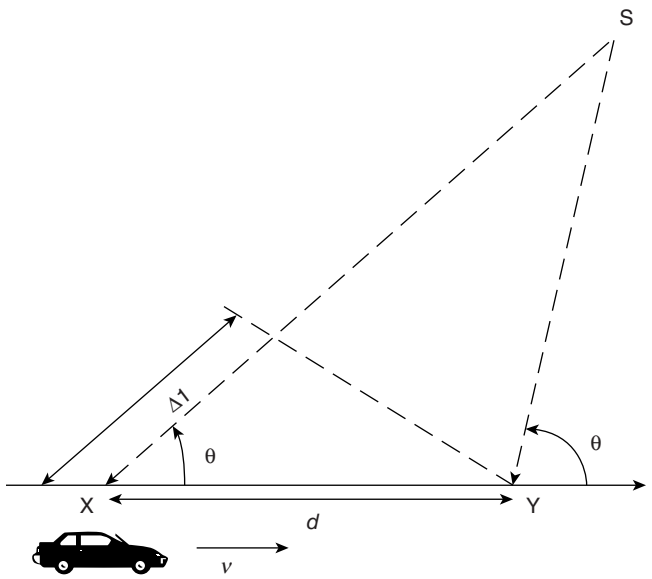

FIGURE 1.3. Geometry of the mobile link for Doppler effect estimation.

source at the current point Y, that is, YS. The phase change of the resultant received signal due to the difference in path lengths is therefore

$$\Delta\Phi = k\Delta\ell = \frac{2\pi}{\lambda}\ell\cos\theta = \frac{2\pi v\Delta t}{\lambda}\cos\theta. \tag{1.11}$$

Hence, the apparent change in frequency radiated, or Doppler shift, is given by f_D, where

$$f_{\mathrm{D}} = \frac{1}{2\pi}\frac{\Delta\Phi}{\Delta t} = \frac{v}{\lambda}\cos\theta. \tag{1.12}$$

It is important to note from Figure 1.3 that the angles θ for points X and Y are the same only when the corresponding lines XS and YS are parallel. Hence, this figure is correct only in the limit when the terminal S is far away from the moving antenna at points X and Y. Many authors have ignored this fact during their geometrical explanation of the Doppler effect [1–4, 10]. Because the Doppler shift is related to the mobile velocity and the spatial angle between the direction of mobile motion and the direction of arrival of the signal, it can be positive or negative depending on whether the mobile receiver is moving toward or away from the transmitter. In fact, from Equation (1.12), if the mobile moves *toward* the direction of arrival of the signal with radiated frequency f_c, then the received frequency is increased; that is, the apparent frequency is $f_{\mathrm{C}} + f_{\mathrm{D}}$. When the mobile moves away from the direction of arrival of the signal, then the received frequency is decreased; that is, the apparent frequency is $f_{\mathrm{C}} - f_{\mathrm{D}}$. The maximum Doppler shift is $f_{\mathrm{Dmax}} = \nu/\lambda$, which in further description will denote simply as f_{m}.

There are many probability distribution functions that can be used to describe the fast fading effects, such as Rayleigh, Suzuki, Rician, gamma, gamma-gamma, and so on. Because the Rician distribution is more general for description of fast fading effects in terrestrial communication links [1–4, 10], as it includes both line-of-sight (LOS) together with scattering and diffraction with non-line-of-sight (NLOS), we briefly describe it in the following paragraph.

To estimate the contribution of each signal component, at the receiver, due to the dominant (or LOS) and the secondary (or multipath), the Rician parameter K is usually introduced, as a ratio between these components [1–4, 10], that is,

$$K = \frac{\text{LOS} - \text{Component power}}{\text{Multipath} - \text{Component power}} \tag{1.13}$$

The Rician PDF distribution of the signal strength or voltage envelope r can be defined as [1–4, 10]:

$$\mathrm{PDF}(r) = \frac{r}{\sigma^2}\exp\left\{-\frac{r^2 + A^2}{2\sigma^2}\right\} I_0\left(\frac{Ar}{\sigma^2}\right), \text{ for } A > 0, r \geq 0, \tag{1.14}$$

where A denotes the peak strength or voltage of the dominant component envelope, σ is the standard deviation of signal envelope, and $I_0(\cdot)$ is the modified Bessel function of the first kind and zero order. According to definition (1.13), we can now rewrite the parameter K, which was defined earlier as the ratio between the *dominant* and the *multipath* component power. It is given by

$$K = \frac{A^2}{2\sigma^2}. \tag{1.15}$$

Using (1.15), we can rewrite (1.14) as a function of K only [1–3, 10]:

$$\mathrm{PDF}(r) = \frac{r}{\sigma^2}\exp\left\{-\frac{r^2}{2\sigma^2}\right\}\exp(-K))I_0\left(\frac{r}{\sigma}\sqrt{2K}\right). \tag{1.16}$$

Using such presentation of Rician PDF, one can easily obtain the mean value and the variance as functions of the parameter K, called also the *fading parameter*. Thus, according to definitions of the mean value and the variance [3, 6], we get

$$\mu_r(K) = \int_0^\infty r \cdot \mathrm{PDF}(r)dr = \left[(1+K)I_0\left(\sqrt{2Kr}\right) + KI_1(K/2)\right] \tag{1.17}$$

and

$$\sigma_r^2(K) = \int_0^\infty r^2 \cdot \mathrm{PDF}(r)dr = 2\cdot(1+K) - \mu_r^2. \tag{1.18}$$

Here, $I_1(\cdot)$ is the modified Bessel function of the first kind and first order.

For $K = 0$, that is, the worst case of the fading channel, in expression (1.16), the term $\exp(-K) = 1$ and $I_0(0) = 1$. This worst-case scenario is described by the Rayleigh PDF, when there is NLOS signal only and it is equal to

$$\mathrm{PDF}(r) = \frac{r}{\sigma^2}\exp\left\{-\frac{r^2}{2\sigma^2}\right\}. \tag{1.19}$$

Conversely, in a situation of good clearance between two terminals with no multipath components, that is, when $K \to \infty$, the Rician fading approaches a Gaussian one, yielding a "Dirac-delta shaped" PDF described by Equation (1.9a) (see Fig. 1.4). We will use these definitions in Chapter 11 for the link budget design inside a terrestrial radio communication system.

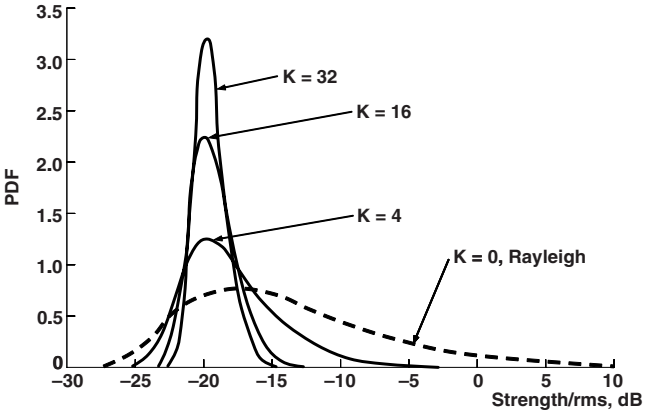

FIGURE 1.4. Rician PDF distribution versus ratio of signal to rms.

Finally, for the practical point of view, we will present the mean and the variance of Rician distribution, respectively. Thus, for $K < 2$, from expression (1.17) it follows, according to Reference 14, that

$$\mu_r(K) = \sqrt{\frac{\pi}{2}} + \sum_{n=1}^{\infty} \frac{2}{\pi} \cdot \frac{(-1)^n}{(2n-1)!} K^n, \tag{1.20a}$$

whereas for $K \geq 2$,

$$\mu_r(K) = \sqrt{2K}\left(1 - \frac{1}{4K} + \frac{1}{K^2}\right). \tag{1.20b}$$

The same approximations can be obtained for the variance following derivations of expression (1.18) made in Reference 14. Thus, for $K < 2$,

$$\sigma_r^2(K) = 1 - \left(\frac{\pi}{2} - 1\right) \cdot \exp\left\{-\frac{K}{\sqrt{2}}\right\}, \tag{1.21a}$$

whereas for $K \geq 2$,

$$\sigma_r^2(K) = 1 - \frac{1}{4K}\left(1 + \frac{1}{K} - \frac{1}{K^2}\right). \tag{1.21b}$$

Using now relations between the PDF and CDF, we can obtain from expression (1.19) the Rayleigh CDF presentation:

$$CDF(R) \equiv \Pr(r \leq R) = \int_0^R PDF(r)dr = 1 - \exp\left\{-\frac{R^2}{2\sigma_r^2}\right\}. \tag{1.22}$$

Now, using (1.16) for the Rician PDF, we have a more difficult equation for Rician CDF with respect to Rayleigh CDF due to summation of an infinite number of terms, such as

$$CDF(R) = 1 - \exp\left\{-\left(K + \frac{r^2}{2\sigma_r^2}\right)\right\} \cdot \sum_{m=0}^{\infty}\left(\frac{\sigma_r\sqrt{2K}}{r}\right) \cdot I_m\left(\frac{r \cdot \sqrt{2K}}{\sigma_r}\right). \quad (1.23)$$

Here $I_m(\cdot)$ is the modified Bessel function of the first kind and mth-order. Once more, the Rician CDF depends on one parameter K only and limits to the Rayleigh CDF and Gaussian CDF for $K = 0$ and for $K \to \infty$, respectively. Clearly, the CDF Equation (1.23) is more complicated to evaluate analytically or numerically than the PDF Equation (1.16). However, in practical terms, it is sufficient to use m up to the value where the last term's contribution becomes less than 0.1%. It was shown in Reference 9 that for a Rician CDF with $K = 2$, the 14-dB fading outage probability is about 10^{-2}.

1.4.3. Signal Presentation in Wireless Communication Channels

To understand how to describe mathematically multipath fading in communication channels, we need to understand what kinds of signals we "deal" with in each channel.

Narrowband (CW) Signals. A voice-modulated CW signal occupies a very narrow bandwidth surrounding the carrier frequency f_c of the radio frequency (RF) signal (e.g., the carrier), which can be expressed as

$$x(t) = A(t)\cos[2\pi f_c t + \varphi(t)], \quad (1.24)$$

where $A(t)$ is the signal envelope (i.e., slowly varied amplitude) and $\varphi(t)$ is its signal phase. For example, for a modulated 1-GHz carrier signal by a signal of bandwidth $\Delta f = 2f_m = 8\ kHz$, the fractional bandwidth is very narrow, that is, $8 \times 10^3\text{Hz}/1\times10^9\text{Hz} = 8 \times 10^{-6}$ or 8×10^{-4}%. Since all information in the signal is contained within the phase and envelope-time variations, an alternative form of a bandpass signal $x(t)$ is introduced [1, 2, 6–10]:

$$y(t) = A(t)\exp\{j\varphi(t)\}, \quad (1.25)$$

which is also called the *complex baseband* representation of $x(t)$. By comparing (1.24) and (1.25), we can see that the relation between the *bandpass* (RF) and the *complex baseband* signals are related by:

$$x(t) = \text{Re}[y(t)\exp(j2\pi f_c t)]. \quad (1.26)$$

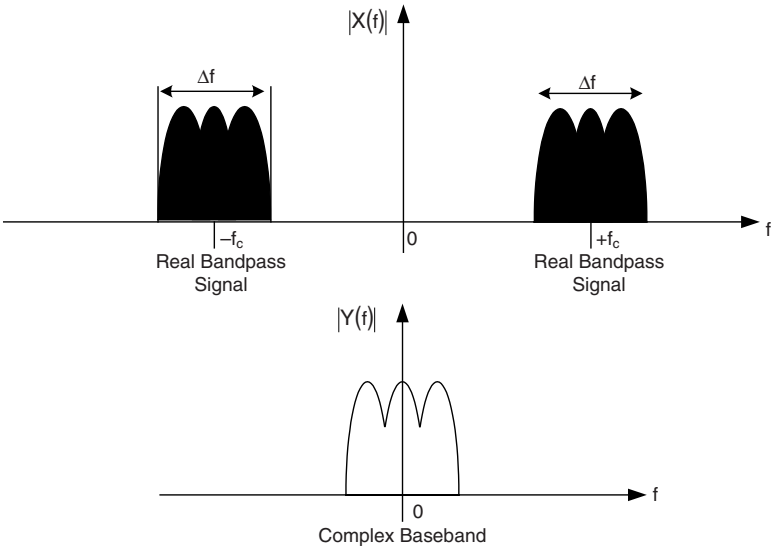

FIGURE 1.5. The signal power presentation in the frequency domain: bandpass (upper figure) and baseband (lower figure).

The relations between these two representations of the narrowband signal in the frequency domain is shown schematically in Figure 1.5. One can see that the complex baseband signal is a frequency-shifted version of the bandpass (RF) signal with the same spectral shape, but centered around a zero frequency instead of the f_c [7]. Here, $X(f)$ and $Y(f)$ are the Fourier transform of $x(t)$ and $y(t)$, respectively, and can be presented in the following manner [1, 2]:

$$Y(f) = \int_{-\infty}^{\infty} y(t)e^{-j2\pi ft}\mathrm{d}t = \mathrm{Re}[Y(f)] + j\,\mathrm{Im}[Y(f)] \tag{1.27}$$

and

$$X(f) = \int_{-\infty}^{\infty} x(t)e^{-j2\pi ft}\mathrm{d}t = \mathrm{Re}[X(f)] + j\,\mathrm{Im}[X(f)]. \tag{1.28}$$

Substituting for $x(t)$ in integral (1.28) from (1.26) gives

$$X(f) = \int_{-\infty}^{\infty} \mathrm{Re}\left[y(t)e^{j2\pi f_c t}\right]e^{-j2\pi ft}\mathrm{d}t. \tag{1.29}$$

Taking into account that the real part of any arbitrary complex variable w can be presented as

$$\mathrm{Re}[w] = \frac{1}{2}[w + w^*]$$

where w^* is the complex conjugate, we can rewrite (1.29) in the following form:

$$X(f) = \frac{1}{2}\int_{-\infty}^{\infty} [y(t)e^{j2\pi f_c t} + y^*(t)e^{-j2\pi f_c t}] \cdot e^{-j2\pi ft}\,\mathrm{d}t. \tag{1.30}$$

After comparing expressions (1.27) and (1.30), we get

$$X(f) = \frac{1}{2}[Y(f - f_c) + Y^*(-f - f_c)]. \tag{1.31}$$

In other words, the spectrum of the real bandpass signal $x(t)$ can be represented by real part of that for the complex baseband signal $y(t)$ with a shift of $\pm f_c$ along the frequency axis. It is clear that the baseband signal has its frequency content centered on the "zero" frequency value.

Now we notice that the mean power of the baseband signal $y(t)$ gives the same result as the mean-square value of the real bandpass (RF) signal $x(t)$, that is,

$$\langle P_y(t)\rangle = \frac{\langle |y(t)|^2 \rangle}{2} = \frac{\langle y(t)y^*(t)\rangle}{2} \equiv \langle P_x(t)\rangle. \tag{1.32}$$

The complex envelope $y(t)$ of the received narrowband signal can be expressed according to (1.25), within the multipath wireless channel, as a sum of phases of N baseband individual multiray components arriving at the receiver with their corresponding time delay, τ_i, $i = 0, 1, 2, \ldots, N-1$ [6–10]:

$$y(t) = \sum_{i=0}^{N-1} u_i(t) = \sum_{i=0}^{N-1} A_i(t)\exp[j\varphi_i(t, \tau_i)]. \tag{1.33}$$

If we assume that during the subscriber movements through the local area of service the amplitude A_i time variations are small enough, whereas phases φ_i vary greatly due to changes in propagation distance between the BS and the desired subscriber, then there are great random oscillations of the total signal $y(t)$ at the receiver during its movement over a small distance. Since $y(t)$ is the phase sum in (1.33) of the individual multipath components, the instantaneous phases of the multipath components result in large fluctuations, that

is, fast fading, in the CW signal. The average received power for such a signal over a local area of service can be presented according to References 1–3 and 6–10 as

$$\langle P_{\mathrm{CW}} \rangle \approx \sum_{i=0}^{N-1} \langle A_i^2 \rangle + 2 \sum_{i=0}^{N-1} \sum_{i,j \neq i} \langle A_i A_j \rangle \langle \cos[\varphi_i - \varphi_j] \rangle. \tag{1.34}$$

Wideband (Pulse) Signals. The typical *wideband* or *impulse* signal passing through the multipath communication channel is shown schematically in Figure 1.6a according to References 1–4. If we divide the time-delay axis into equal segments, usually called bins, then there will be a number of received signals, in the form of vectors or delta functions. Each bin corresponds to a different path whose time of arrival is within the bin duration, as depicted in Figure 1.6b. In this case, the time-varying discrete-time impulse response can be expressed as

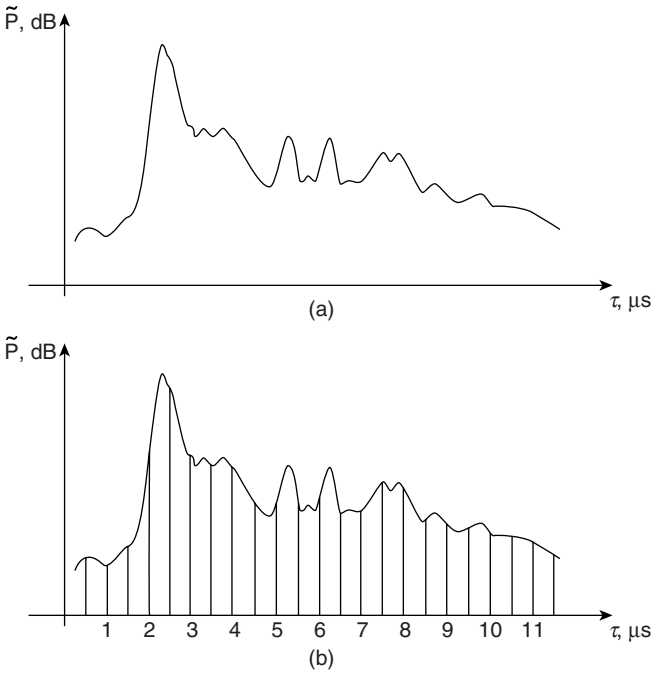

FIGURE 1.6. (a) A typical impulse signal passing through a multipath communication channel according to References 1–4. (b) The use of bins, as vectors, for the impulse signal with spreading.

$$h(t,\tau)=\left\{\sum_{i=0}^{N-1}A_i(t,\tau)\exp[-j2\pi f_c\tau_i(t)]\delta(\tau-\tau_i(t))\right\}\exp[-j\varphi(t,\tau)]. \qquad (1.35)$$

If the channel impulse response is assumed to be time invariant, or is at least stationary over a short-time interval or over a small-scale displacement of the receiver/transmitter, then the impulse response (1.35) reduces to

$$h(t,\tau)=\sum_{i=0}^{N-1}A_i(\tau)\exp[-j\theta_i]\delta(\tau-\tau_i), \qquad (1.36)$$

where $\theta_i = 2\pi f_c\tau_i + \varphi(\tau)$. If so, the received power delay profile for a wideband or pulsed signal averaged over a small area can be presented simply as a sum of the powers of the individual multipath components, where each component has a random amplitude and phase at any time, that is,

$$\langle P_{pulse}\rangle=\left\langle\sum_{i=0}^{N-1}\{A_i(\tau)|\exp[-j\theta_i]|\}^2\right\rangle\approx\sum_{i=0}^{N-1}\langle A_i^2\rangle. \qquad (1.37)$$

The received power of the wideband or pulse signal does not fluctuate significantly when the subscriber moves within a local area, because in practice, the amplitudes of the individual multipath components do not change widely in a local area of service.

Comparison between small-scale presentations of the average power of the narrowband (CW) and wideband (pulse) signals, that is, (1.34) and (1.37), shows that when $\langle A_iA_j\rangle = 0$ or/and $\langle\cos[\varphi_i - \varphi_j]\rangle = 0$, the average power for CW signal and that for pulse are equivalent. This can occur when either the path amplitudes are uncorrelated, that is, each multipath component is independent after multiple reflections, diffractions, and scattering from obstructions surrounding both the receiver and the transmitter or the BS and the subscriber antenna. It can also occur when multipath phases are independently and uniformly distributed over the range of $[0.\,2\pi]$. This property is correct for UHF/X-wavebands when the multipath components traverse differential radio paths having hundreds of wavelengths [6–10].

1.4.4. Parameters of the Multipath Communication Channel

So the question that remains to be answered is which kind of fading occurs in a given wireless channel.

Time Dispersion Parameters. First, we need to mention some important parameters for wideband (pulse) signals passing through a wireless channel. These parameters are determined for a certain threshold level X (in dB) of the channel under consideration and from the signal power delay profile. These

parameters are the mean excess delay, the rms delay spread, and the excess delay spread.

The *mean excess delay* is the first moment of the power delay profile of the pulse signal and is defined as

$$\langle \tau \rangle = \frac{\sum_{i=0}^{N-1} A_i^2 \tau_i}{\sum_{i=0}^{N-1} A_i^2} = \frac{\sum_{i=0}^{N-1} P(\tau_i)\tau_i}{\sum_{i=0}^{N-1} P(\tau_i)}. \tag{1.38}$$

The *rms delay spread* is the square root of the second central moment of the power delay profile and is defined as

$$\sigma_\tau = \sqrt{\langle \tau^2 \rangle - \langle \tau \rangle^2}, \tag{1.39}$$

where

$$\langle \tau^2 \rangle = \frac{\sum_{i=0}^{N-1} A_i^2 \tau_i^2}{\sum_{i=0}^{N-1} A_i^2} = \frac{\sum_{i=0}^{N-1} P(\tau_i)\tau_i^2}{\sum_{i=0}^{N-1} P(\tau_i)}. \tag{1.40}$$

These delays are measured relative to the first detectable signal arriving at the receiver at $\tau_0 = 0$. We must note that these parameters are defined from a single power delay profile, which was obtained after temporal or local (small-scale) spatial averaging of measured impulse response of the channel [1–3, 7–10].

Coherence Bandwidth. The power delay profile in the time domain and the power spectral response in the frequency domain are related through the Fourier transform. Hence, to describe a multipath channel in full, both the delay spread parameters in the time domain and the *coherence bandwidth* in the frequency domain are used. As mentioned earlier, the coherence bandwidth is the statistical measure of the frequency range over which the channel is considered "flat." In other words, this is a frequency range over which two frequency signals are strongly amplitude correlated. This parameter, actually, describes the time-dispersive nature of the channel in a small-scale (local) area. Depending on the degree of amplitude correlation of two frequency separated signals, there are different definitions for this parameter.

The first definition is the *coherence bandwidth*, B_c, which describes a bandwidth over which the frequency correlation function is above 0.9 or 90%, and it is given by

$$B_c \approx 0.02\sigma_\tau^{-1}. \tag{1.41}$$

The second definition is the *coherence bandwidth*, B_c, which describes a bandwidth over which the frequency correlation function is above 0.5 or 50%, or

$$B_c \approx 0.2\sigma_\tau^{-1}. \tag{1.42}$$

There is not any single exact relationship between coherence bandwidth and rms delay spread, and expressions (1.41) and (1.42) are only approximate equations [1–6, 7–10].

Doppler Spread and Coherence Time. To obtain information about the time-varying nature of the channel caused by movements, from either the transmitter/receiver or scatterers located around them, new parameters, such as the *Doppler spread* and the *coherence time*, are usually introduced to describe the time variation phenomena of the channel in a small-scale region. The Doppler spread B_D is defined as a range of frequencies over which the received Doppler spectrum is essentially nonzero. It shows the spectral spreading caused by the time rate of change of the mobile radio channel due to the relative motions of vehicles (and scatterers around them) with respect to the BS. According to References 1–4 and 7–10, the Doppler spread B_D depends on the Doppler shift f_D and on the angle α between the direction of motion of any vehicle and the direction of arrival of the reflected and/or scattered waves (see Fig. 1.3). If we deal with the complex baseband signal presentation, then we can introduce the following criterion: If the baseband signal bandwidth is greater than the Doppler spread B_D, the effects of Doppler shift are negligible at the receiver.

Coherence time T_c is the time domain dual of Doppler spread, and it is used to characterize the time-varying nature of the frequency dispersiveness of the channel in time coordinates. The relationship between these two-channel characteristics is

$$T_c \approx \frac{1}{f_m} = \frac{\lambda}{v}. \tag{1.43}$$

We can also define the coherence time according to References 1–4 and 7–10 as the time duration over which two multipath components of the received signal have a strong potential for amplitude correlation. One can also define the coherence time as the time over which the correlation function of two different signals in the time domain is above 0.5 (or 50%). Then, according to References 7 and 10, we get

$$T_c \approx \frac{9}{16\pi f_m} = \frac{9\lambda}{16\pi v} = 0.18\frac{\lambda}{v}. \tag{1.44}$$

This definition is approximate and can be improved for modern digital communication channels by combining Equations (1.43) and (1.44) to get:

$$T_c \approx \frac{0.423}{f_m} = 0.423\frac{\lambda}{v}. \tag{1.45}$$

The definition of coherence time implies that two signals arriving at the receiver with a time separation greater than T_c are affected differently by the channel.

1.4.5. Types of Fading in Multipath Communication Channels

Let us now summarize the effects of fading, which may occur in static or dynamic multipath communication channels.

Static Channel. In this case, multipath fading is purely spatial and leads to constructive or destructive interference at various points in space at any given instant in time, depending on the relative phases of the arriving signals. Furthermore, fading in the frequency domain does not change because the two antennas are stationary. The signal parameters of interest, such as the signal bandwidth, B_s, the time of duration, T_s, with respect to the coherent time, T_c, and the coherent bandwidth, B_c, of the channel are shown in Figure 1.7. There are two types of fading that occur in static channels:

A. Flat Slow Fading (FSF) (see Fig. 1.8), where the following relations between *signal* parameters of the signal and a channel are valid [7–10]:

$$T_c >> T_S; \quad B_D \cong 0 << B_S; \quad \sigma_\tau < T_S; \quad B_c \sim \frac{0.02}{\sigma_\tau} > B_S \tag{1.46}$$

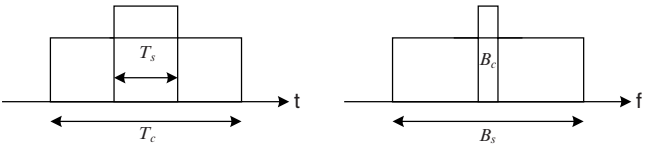

FIGURE 1.7. Comparison between signal and channel parameters.

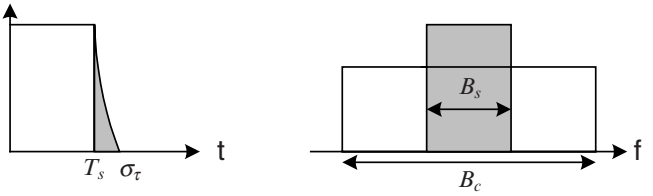

FIGURE 1.8. Relations between parameters for flat slow fading.

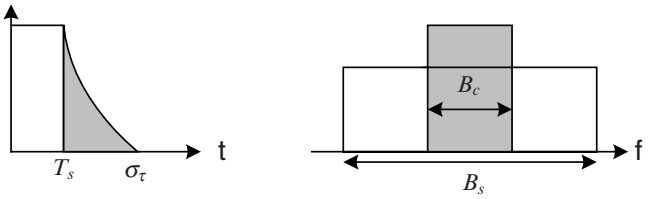

FIGURE 1.9. Relations between parameters for flat fast fading.

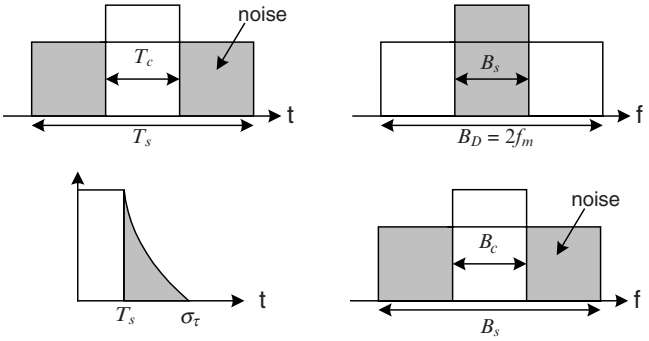

FIGURE 1.10. Relations between parameters for frequency selective fast fading.

Here all harmonics of the total signal are coherent.

B. Flat Fast Fading (FFF) (see Fig. 1.9), where the following relations between the parameters of a channel and the signal are valid [7–10]:

$$T_c >> T_S; \quad B_D \cong 0 << B_S; \quad \sigma_\tau > T_S; \quad B_c < B_S \tag{1.47}$$

Dynamic Channel. There are two additional types of fading that occur in a dynamic channel.

A. Frequency Selective Fast Fading (FSFF) (see Fig. 1.10), when fast fading depends on the frequency. In this case, following relations between the parameters of a channel and the signal are valid [7–10]:

$$T_c < T_S; \quad B_D > B_S; \quad \sigma_\tau > T_S; \quad B_c < B_S \tag{1.48}$$

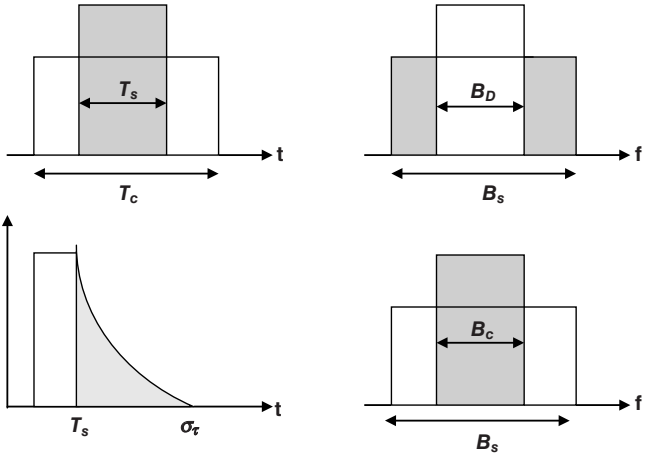

FIGURE 1.11. Relations between parameters for frequency selective slow fading.

B. Frequency Selective Slow Fading (FSSF) (see Fig. 1.11), when slow fading depends on the frequency. In this case, following relations between the parameters of a channel and the signal are valid [7–10]:

$$T_c > T_S; \quad B_D < B_S; \quad \sigma_\tau > T_S; \quad B_c < B_S \tag{1.49}$$

Using these relationships between the parameters of the signal and that of a channel, we can define, a priori, the type of fading mechanism which may occur in a wireless communication link (see Fig. 1.12).

1.4.6. Characterization of Multipath Communication Channels with Fading

In previous subsections, we described situations that occur in real communication channels, where natural propagation effects for each specific environment are very actual. Namely, as will be shown in Chapter 13, the ionospheric channel can be considered as a time-varying channel due to scattering from the ionosphere (see Fig. 1.13). Thus, in the ionosphere, due to plasma movements, the parameters of fading have a dispersive character—time dispersive or frequency dispersive. The same effects of the multiplicative noise will be analyzed in Chapter 14 for the land-to-satellite communication channel.

We present another example of terrestrial multipath channel (see Chapters 5 and 8), caused by multipath propagation of rays reflected from building walls (see Fig. 1.14a), diffracted from a hill (see Fig. 1.14b), and scattered from a tree (see Fig. 1.14c). All these channels we define as *time-varying* or *frequency-varying* multipath channels with fading depend on their "reaction" of the propagating radio wave with the environment. Thus, in land communication channels due to multiple scattering and diffraction, the channel becomes fre-

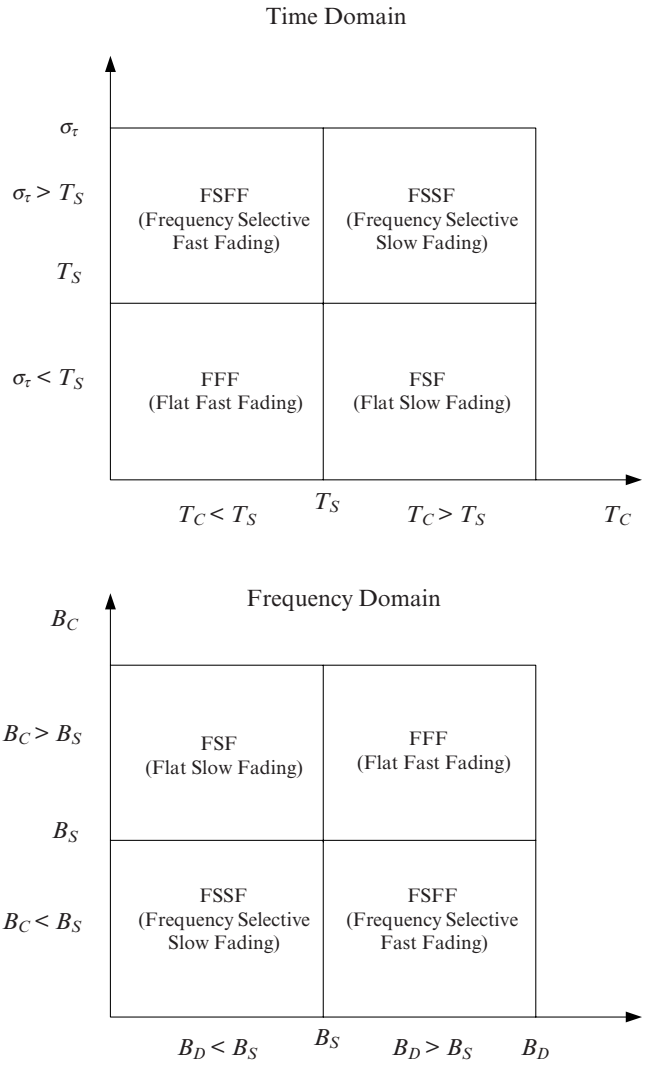

FIGURE 1.12. Common picture of different kinds of fading, depending on relations between the signal and the channel main parameters.

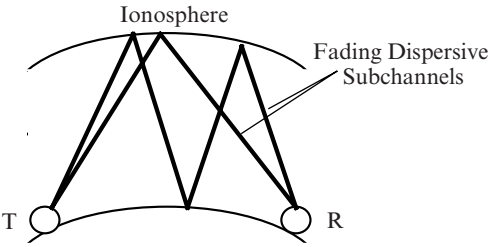

FIGURE 1.13. Multipath phenomena in the land–ionospheric link.

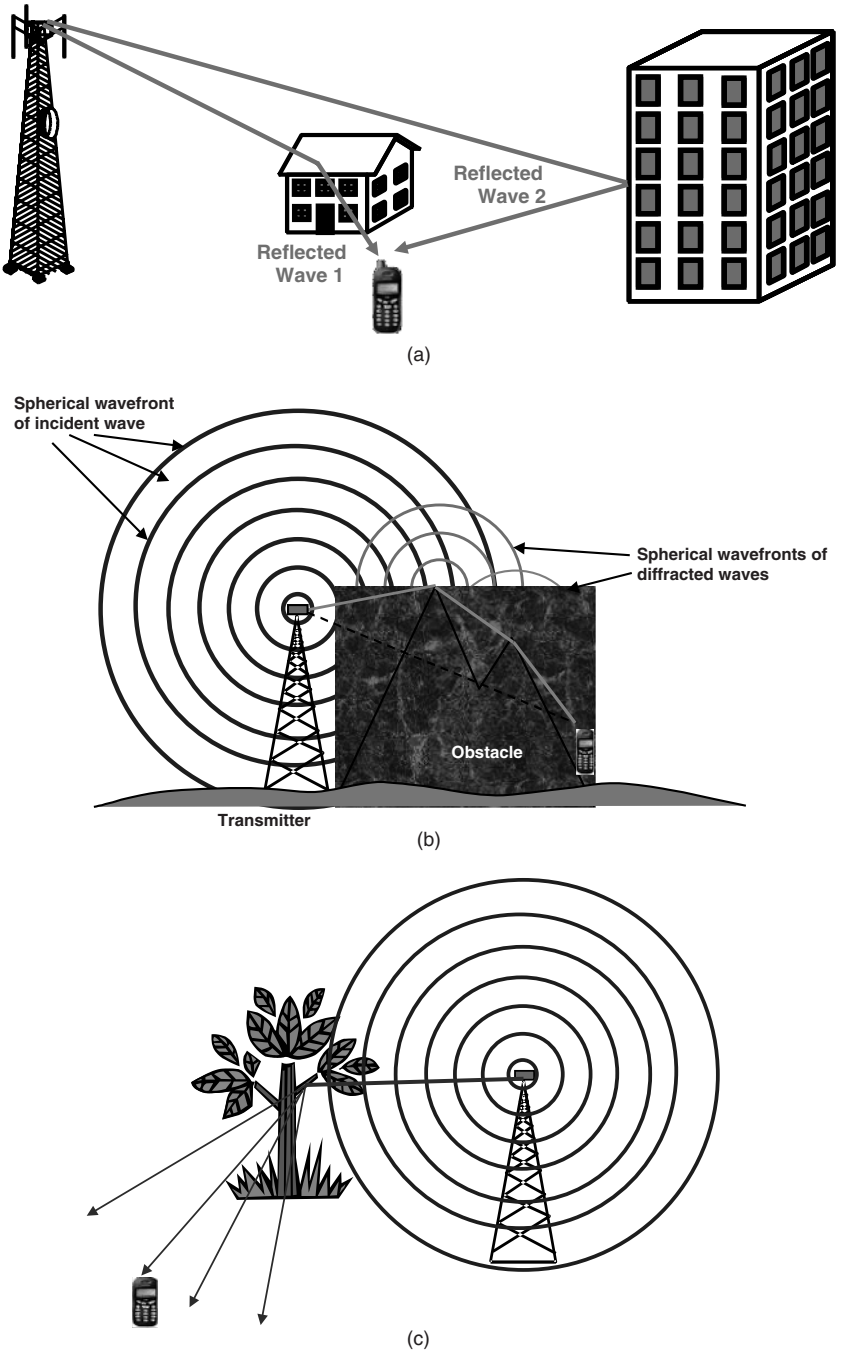

FIGURE 1.14. (a) Specular reflection from walls and roofs. (b) Multiple diffraction from hills. (c) Multiple scattering from tree's leaves.

quency selective. If one of the antennas is moving—mostly the subscriber (MS) antenna—the channel is a *time-dispersive* channel. For the case of a stationary receiver and transmitter (defined earlier as a *static* multipath channel), due to multiple reflections and scattering from various obstructions surrounding the BS and subscriber antennas, we obtain the signal spread with a standard deviation of σ_τ in the time domain as shown in Figure 1.15. As a result, radio signals traveling along different paths of varying lengths cause significant deviations of the signal strength (in volts) or signal power (in watts) at the receiver. This interference picture is not changed in time and can be repeated in each phase of radio communication between the BS and the stationary subscriber (see Fig. 1.16). In the case of a *dynamic* channel, described in the previous subsection, either the subscriber antenna is moving or the objects surrounding the stationary antennas move and the spatial variations of the resultant signal at the receiver can be seen as temporal variations, as the receiver moves

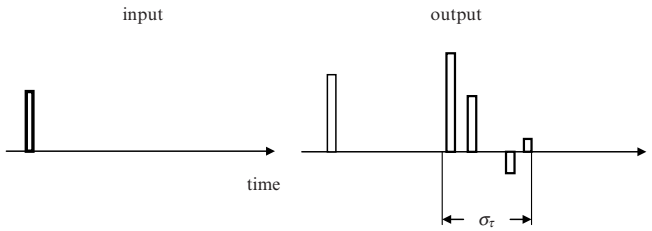

FIGURE 1.15. The multipath delay spread σ_τ in the time-invariant (stationary) channel.

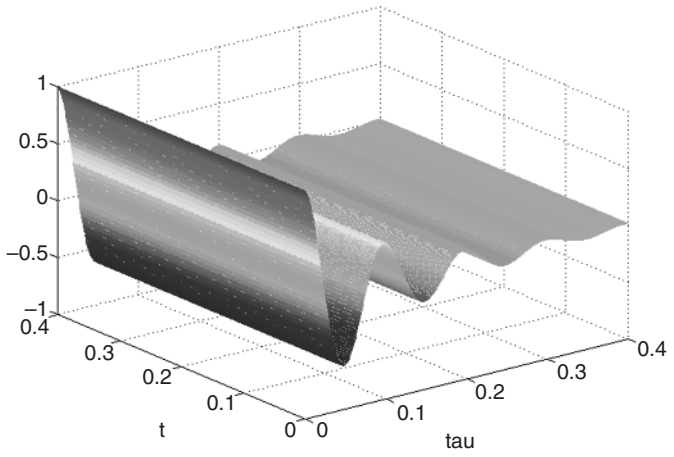

FIGURE 1.16. Time-invariant or stationary channel.

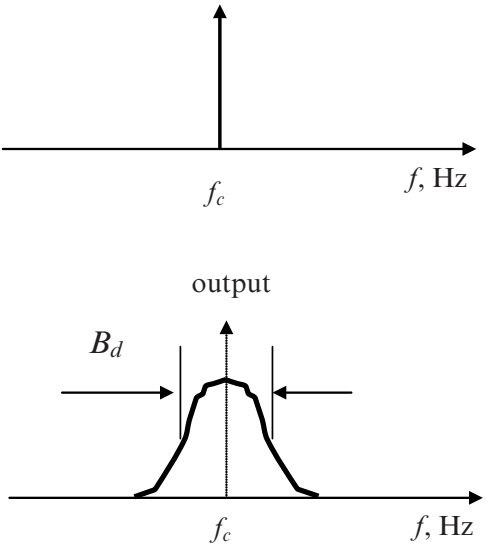

FIGURE 1.17. Doppler spread caused by mobile subscriber.

through the multipath field (i.e., through the interference picture of the field pattern). In such a dynamic multipath channel, signal fading at the mobile receiver occurs in the time domain. This temporal fading relates to a shift of frequency radiated by the stationary transmitter (see Fig. 1.17). In fact, the time variations, or dynamic changes of the propagation path lengths, are related to the Doppler shift, denoted earlier by $f_{d\max}$, which is caused by the relative movements of the stationary BS and the MS. The total bandwidth due to Doppler shift is $B_d = 2f_{d\max}$. In the time-varied or dynamic channel, in any real time t, there is no repetition of the interference picture during crossing of different field patterns by the MS at each discrete time of his movements, as shown in Figure 1.18.

1.5. HIGH-LEVEL FADING STATISTICAL PARAMETERS

In real situations in mobile communications, when conditions in dynamic channels are more realistic (see Fig. 1.12), due to the motion of the receiver or the transmitter, the picture of envelope fading varies. In such realistic scenarios occurring in the urban environment, the fading rate and the signal envelope amplitude are functions of time. If so, for the wireless network designers, it is very important to obtain at the quantitative level a description of the rate, at which fades of any depth occur and of the average duration of a fade below

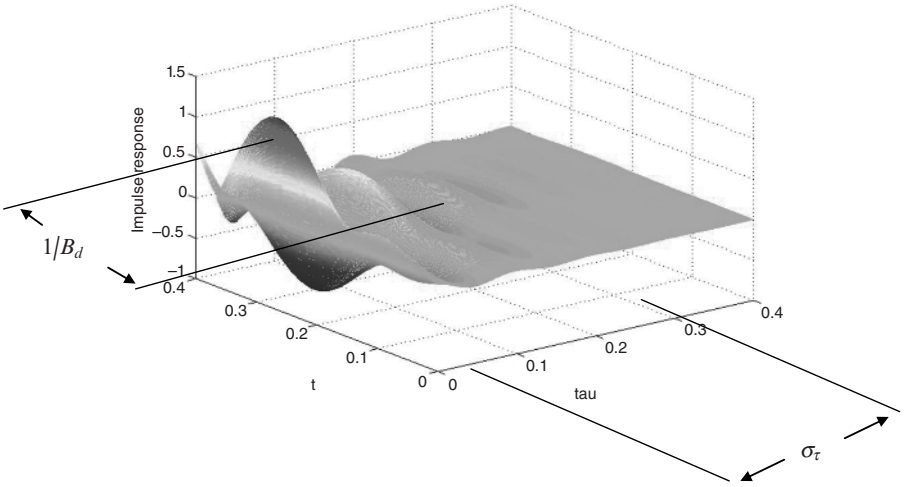

FIGURE 1.18. Time-varying or dynamic channel.

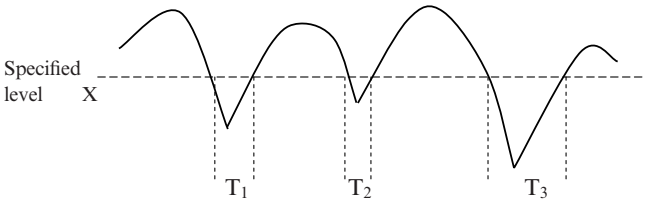

FIGURE 1.19. The illustration of definitions of the signal fading statistical parameters LCR and AFD.

any given depth (usually called the sensitivity or the threshold of the receiver input). Therefore, there are two important high-level statistical parameters of a fading signal, the *level crossing rate* (LCR) and the *average fade duration* (AFD) that are usually introduced in the literature. These parameters are useful for mobile link design and, mostly, for designing various coding protocols in wireless digital networks, where the required information is provided in terms of LCR and AFD.

The manner in which both required parameters, LCR and AFD, can be defined is illustrated in Figure 1.19. As shown in Figure 1.19, the LCR at any specified threshold (i.e., a sensitivity level of the receiver) X is defined as the expected rate at which the received signal envelope crosses that level in a

positive-going or negative-going direction. To find this expected rate, we need information about the joint PDF of the specific level X and the slope of the envelope curve $r(t)$, $\dot{r} = dr/dt$, that is, about PDF(X, $\dot{r}$). The same should be done to define AFD, defined as the average period of time for which the receiver signal envelope is below a specific threshold X (see Fig. 1.19).

1.5.1. Level Crossing Rate: A Mathematical Description

Rayleigh Fading Channel. In terms of this joint PDF, the LCR is defined as the expected rate at which the Rayleigh fading envelope, normalized to the local *rms* signal level, crosses a specified level X, let us say in a positive-going direction. The number of level crossings per second, or the LCR, N_x can be obtained, using the following definition [1, 4, 5]:

$$N_X = \int_0^\infty \dot{r} \cdot PDF(X, \dot{r}) d\dot{r} = \sqrt{2\pi} f_m \zeta \exp\left(-\zeta^2\right), \tag{1.50}$$

where, as above, $f_m = \nu/\lambda$ is the maximum Doppler frequency shift and

$$\zeta = \frac{X}{\sqrt{2} \cdot \sigma_r} \equiv \frac{X}{rms} \tag{1.51}$$

is the value of specific level X, normalized to the local *rms* amplitude of fading envelope (according to Rayleigh statistics $rms = \sqrt{2} \cdot \sigma_r$, see Section 1.4.2). Because f_m is a function of mobile speed v, the value N_x also depends, according to (1.50), on this parameter. For deep Rayleigh fading, there are few crossings at both high and low levels [1–4] with the maximum rate occurring at $\zeta = 1/\sqrt{2}$, that is, at the level 3 dB below the *rms* level.

Rician Fading Channel. In this case, the number of level crossings per second, or the LCR, N_x, can be obtained, using the following result obtained from Reference 13:

$$\begin{aligned} N_X(X) = \int_0^\infty \dot{r} \cdot PDF(X, \dot{r}) d\dot{r} &= \frac{2X\sqrt{2\varsigma}}{\pi^{3/2} \mathrm{K}(0)} e^{-(X^2+\rho^2)/\mathrm{K}(0)} \\ &\times \int_0^{\pi/2} \cosh\left(\frac{2X\rho\cos\alpha}{\mathrm{K}(0)}\right) \left[e^{-\xi\rho\sin\alpha} + \sqrt{\pi}\xi\rho\sin\alpha Q(\xi\rho\sin\alpha)\right] d\alpha. \end{aligned} \tag{1.52}$$

Here, as above, X denotes the level of the receiver input; $\rho \equiv |y(t)| = [K/(K+1)]^{1/2}$ is the amplitude of the LOS component of the signal strength; $\mathrm{Q}(w)$

is the error function from (1.10); $\varsigma = -\frac{1}{2}\mathrm{K}''(0) - \mathrm{Im}\{\mathrm{K}'(0)\}^2 / 2\mathrm{K}(0)$ and $\xi = \left[\omega_D \cos\alpha_0 - \mathrm{Im}\left\{\mathrm{K}'(0)\right\} / \mathrm{K}(0)\right] / \sqrt{2\varsigma}$, where functions $\mathrm{K}(0), \mathrm{K}'(0)$, and $\mathrm{K}''(0)$ are defined in Reference 13 as

$$\mathrm{K}(0) = \frac{1}{K+1} \tag{1.53}$$

$$\mathrm{K}'(0) = -\frac{i\omega_D}{K+1}\left[\frac{\cos\theta \cdot I_1(\kappa)}{I_0(\kappa)}\right] \tag{1.54}$$

$$\mathrm{K}''(0) = \frac{\omega_D^2}{2(K+1)}\left[1 + \frac{\cos 2\theta \cdot I_2(\kappa)}{I_0(\kappa)}\right], \tag{1.55}$$

where $I_n(\kappa)$, $n = 1, 2, 3, \ldots$, are the nth order modified Bessel functions of the first kind, κ determines the beamwidth of arriving waves, and θ denotes the angle between the average scattering direction and the mobile vehicle direction.

Equation (1.52) is a general expression for the envelope LCR and contains (1.50) as a special case of Rayleigh fading, usually used for Doppler effect estimation through the LCR estimates [1, 4, 5].

1.5.2. Average Fade Duration: A Mathematical Description

The AFD, $\langle\tau\rangle$, is defined as the average period of time for which the received signal envelope is below a specific level X (see Fig. 1.19). Its relation with LCR is following

$$\langle\tau\rangle = \frac{1}{N_X} CDF(X). \tag{1.56}$$

Here CDF(X) describes the probability of the event that the received signal envelope $r(t)$ does not exceed a specific level X, that is,

$$CDF(X) \equiv \Pr(r \le X) = \frac{1}{T}\sum_{i=1}^{n} T_i. \tag{1.57}$$

Here T_i is the duration of the fade (see Fig. 1.19) and T is the observation interval of the fading signal.

Rayleigh Fading Statistics. According to the Rayleigh PDF defined by (1.19) and CDF defined by (1.22), the AFD can be expressed, according to (1.56), as a function of ζ and f_m in terms of the *rms* value:

$$\langle \tau \rangle = \frac{\exp(\zeta^2) - 1}{\sqrt{2\pi} f_m \zeta}. \tag{1.58}$$

Rician Fading Statistics. Using relation (1.56) between LCR and AFD, as well as equation (1.52) for $N_x(X)$, one can easily investigate the average fade duration using general Rician fading statistics. We will not present these expressions due to their complexity and will refer the reader to the original work in Reference 13.

We also note that it is very important to determine the rate at which the input signal inside the mobile communication link falls below a given level X, and how long it remains below this level. This is useful for relating the SNR (or S/N), during fading, to the instantaneous *bit error rate* (BER). To someone interested in digital systems design, we point out that knowing the average duration of a signal fade helps to determine the most likely number of signal bits that may be lost during this fading. LCR and AFD primarily depend on the speed of the mobile and decrease as the maximum of Doppler shift becomes larger. An example on how to estimate BER using LCR and AFD will be shown in Chapter 11.

1.6. ADAPTIVE ANTENNAS APPLICATION

The main problem with land communication links is estimating the ratio between the coherent and multipath components of the total signal, that is, the Rician parameter K, to predict the effects of multiplicative noise in the channel of each subscriber located in different conditions in the terrestrial environment. This is shown in Figure 1.20 for various subscribers numbered by $i = 1, 2, 3, \ldots$

However, even a detailed prediction of the radio propagation situation for each subscriber cannot completely resolve all issues of effective service and increase the quality of data stream sent to each user. For this purpose, in present and future generations of wireless systems, adaptive or smart antenna systems are employed to reduce interference and decrease the BER. This topic will be covered in detail in Chapters 7, 8, and 11. Here, in Figure 1.21, we present, schematically, the concept of adaptive (smart) antennas, which allows each mobile subscriber to obtain individual service without inter-user interference and by eliminating multipath phenomena caused by multiple rays arriving to his antenna from various directions.

Even with adaptive/smart antennas (see description in Chapter 7), we cannot totally cancel the effects of the environment, especially in urban areas, due to the spread of the narrow antenna beam both in azimuth and elevation domains caused by an array of buildings located at the rough terrain (see Fig. 1.22). Furthermore, if the desired user is located in a shadow zone with respect to the BS antenna, we may expect the so-called masking effect due to guiding effect of crossing straight streets as shown schematically in Figure 1.23. Thus,

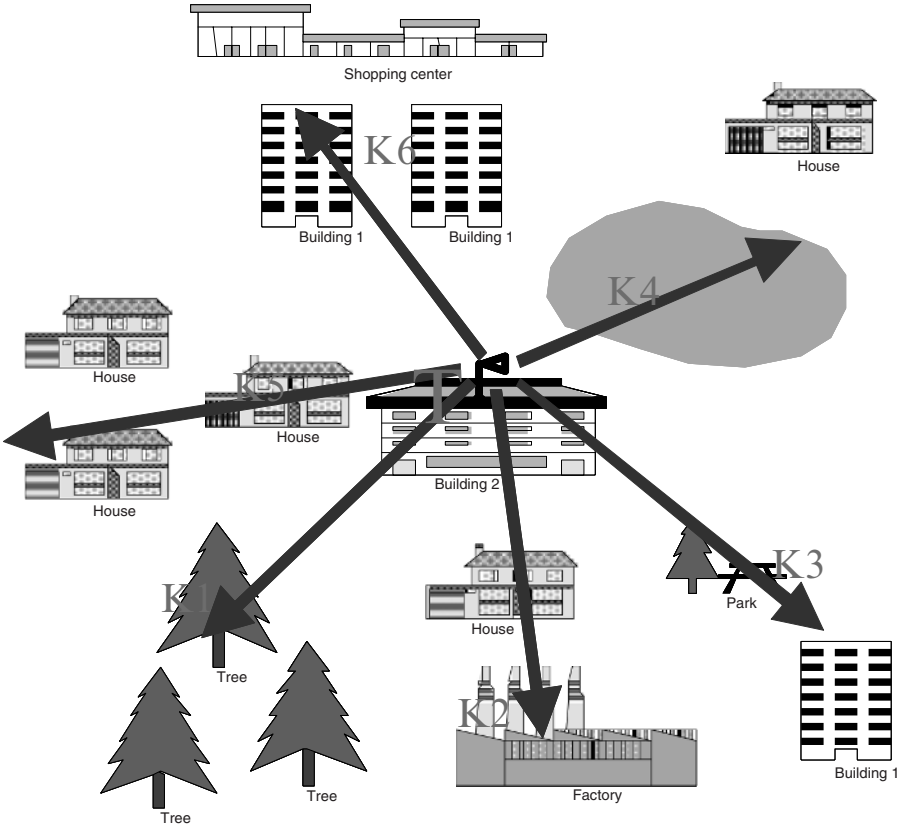

FIGURE 1.20. Scheme of various scenarios in urban communication channel.

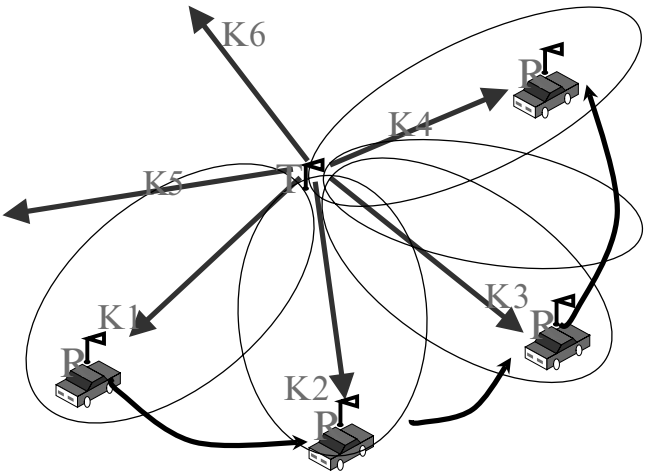

FIGURE 1.21. A scheme for using adaptive antennas for each user located in different conditions in a service area.

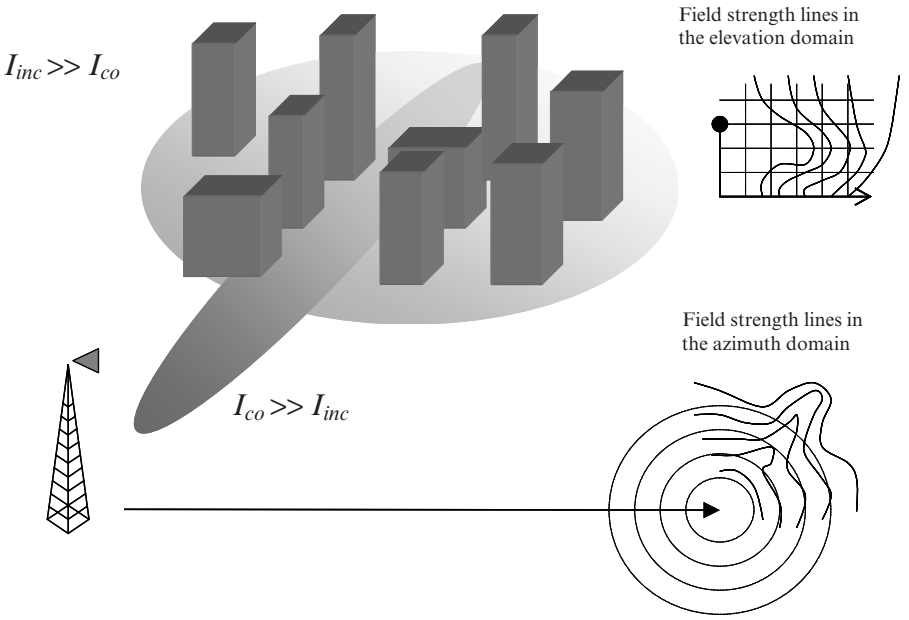

FIGURE 1.22. Effect of built-up area on a narrow-beam adaptive antenna pattern.

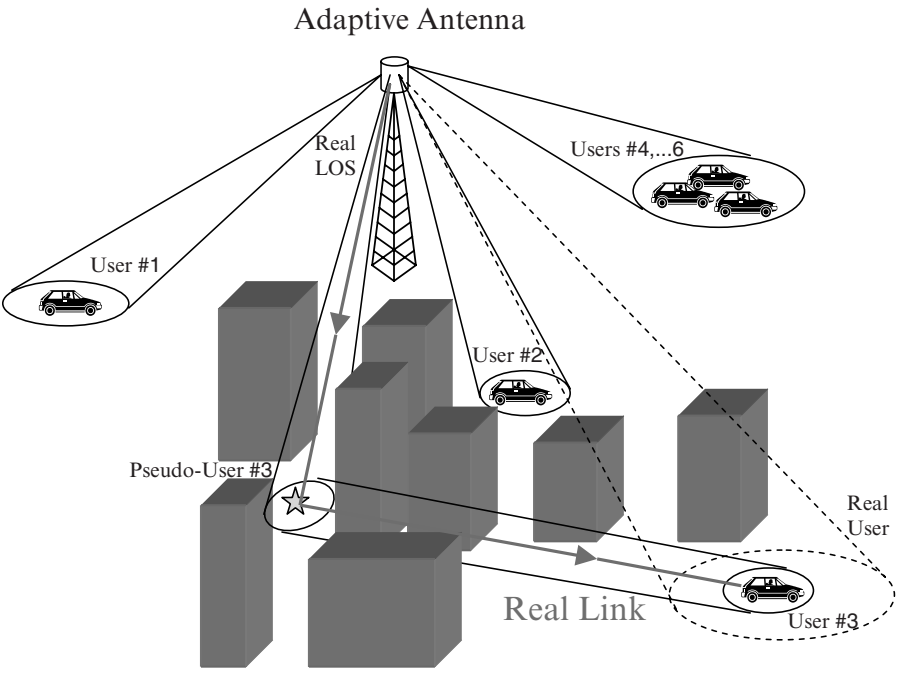

FIGURE 1.23. Street "masking" effect for servicing user #3 by an adaptive antenna.

instead of the real position of user #3, for the adaptive antenna located at the BS, the "real position" will be at the intersection of two straight crossing streets due to guiding effect and channeling of signal energy transmitted by BS antenna along these two streets. Chapters 5 and 8 will focus on terrain effects where a rigorous analysis of these effects on the wireless systems design will be presented.

REFERENCES

1 Jakes, W.C., *Microwave Mobile Communications*, John Wiley & Sons, New York, 1974.

2 Steele, R., *Mobile Radio Communication*, IEEE Press, New York, 1992.

3 Stuber, G.L., *Principles of Mobile Communications*, Kluwer Academic Publishers, Boston-London, 1996.

4 Lee, W.Y.C., *Mobile Cellular Telecommunications Systems*, McGraw Hill, New York, 1989.

5 Molisch, A.F., *Wireless Communications*, Wiley and Sons, London, 2006.

6 Yacoub, M.D., *Foundations of Mobile Radio Engineering*, CRC Press, New York, 1993.

7 Saunders, S.R., *Antennas and Propagation for Wireless Communication Systems*, John Wiley & Sons, New York, 1999.

8 Bertoni, H.L., *Radio Propagation for Modern Wireless Systems*, Prentice Hall PTR, Upper Saddle River, NJ, 2000.

9 Blaunstein, N., "Wireless Communication Systems," in *Handbook of Engineering Electromagnetics*, R. Bansal, ed., Marcel Dekker, New York, 2004.

10 Rappaport, T.S., *Wireless Communications*, Prentice Hall PTR, New York, 1996.

11 Leon-Garcia, A., *Probability and Random Processes for Electrical Engineering*, Addison-Wesley Publishing Company, New York, 1994.

12 Stark, H. and J.W. Woods, *Probability, Random Processes, and Estimation Theory for Engineers*, Prentice Hall, Englewood Cliffs, NJ, 1994.

13 Tepedelenlioglu, C., et al., "Estimation of Doppler spread and spatial strength in mobile communications with applications to handoff and adaptive transmissions," *J Wireless Communic. Mobile Computing*, Vol. 1, No. 2, 2001, pp. 221–241.

14 Krouk, E. and S. Semionov, eds., *Modulation and Coding Techniques in Wireless Communications*, Wiley & Sons, Chichester, England, 2011.